

Power System Voltage Stability of Saudi Arabia Distribution Network as Affected by Large-scale Photovoltaic Power Penetration

ABDELAZIZ SALAH SAIDI¹, LINA ALHMOUD², ADEL ALI ALQAHTANID³
QUCO C'CNKZEMIE⁴, MUHAMMAD UMAR MALIK⁵

¹ Université de Tunis El Manar, École Nationale d'Ingénieurs de Tunis, LR11ES15 Laboratoire des Systèmes Electriques, 1002, Tunis, TUNISIE.

² Department of Electrical Power Engineering, Yarmouk University, Irbid 21163, JORDAN.

³ Saudi Electricity Company, Network Primary Distribution Department - South Operation Area, KSA.

⁴ National Grid company, Project Management Office - Central Operation Area, KSA.

⁵ Sr. Power systems Engineer of Power System Experts, Lahore, PAKISTAN.

Abstract: – Photovoltaic (PV) systems are becoming more prevalent globally, especially in power distribution networks. However, their intermittent integration into these networks can pose reliability concerns regarding voltage instability. Voltage instability is a significant threat to the secure operation of power systems worldwide. With the rise of grid-connected renewable energy-based generation for economic and environmental reasons, there's a growing interest in understanding its impact on voltage stability. This study focuses on assessing and analyzing the effect of 300 MW large-scale PV generation on the voltage stability of the power system, utilizing a comprehensive model tailored to a typical Saudi power grid network. Various performance metrics, including static power flow analysis, PV, and Q-V curves, are employed to analyze how PV generators affect power system static voltage stability. The investigation identifies the maximum permissible PV penetration as 462 MW. Under normal conditions, static load-flow analysis reveals that the highest active and reactive power loss occurs at the transmission lines closest to the solar PV bus. Time domain simulations further corroborate these findings. This work emphasizes the significance of voltage/var control capacity in preserving voltage stability, a feature often deficient in PV systems. It points out that regulating the voltage of PV systems could result in over-voltage concerns, potentially leading to sudden voltage collapse, especially with high regional PV penetration. Nevertheless, the integration of 300 MW large-scale PV demonstrates promising results in static analysis, showcasing reductions in system losses and increased maximum loading capacity of transmission lines.

Key-words: Static voltage stability, Large-scale Solar Photovoltaics, Load flow analysis, Distribution power system, PV-QV curve method, maximum PV penetration level.

Received: March 21, 2024. Revised: September 2, 2024. Accepted: September 21, 2024. Published: October 17, 2024.

1. Introduction

The worldwide rise in renewable energy sources (RES) for generating electricity is evident, propelled by economic and environmental considerations [1-2]. Recent studies highlight the increasing commercial attractiveness of photovoltaic (PV) generation due to its abundant nature, low maintenance requirements, and silent operation [3]. Progress in power electronic interfaces, combined with declining component expenses of PV generators and continuous government incentive programs, has substantially reduced the overall deployment expenses of PV energy sources. Consequently, this has catalyzed increased integration of solar energy into grids across the

globe, aiming to reduce energy costs. For instance, The Saudi government has pinpointed more than 35 sites for renewable energy initiatives, primarily emphasizing solar photovoltaic, wind, and concentrated solar power (CSP) projects [4-6]. These initiatives align with the long-term targets of Vision 2030. As part of this vision, the government plans to complete several renewable energy projects by 2030, with approximately 3.1 GW of total capacity, including 2.2 GW from solar PV and 0.9 GW from wind energy [7-8]. Particularly, leveraging private-sector investment and fostering public-private partnerships are vital strategies for effectively managing the nation's power requirements. A standout example of this approach is the Sakaka Solar PV project, initiated by Saudi Arabia's Renewable Energy Development Office (REPDO), which represents a cornerstone in the country's

energy diversification and development efforts. Its successful completion represents a significant milestone, accompanied by agreements for seven additional solar power projects across various locations, collectively contributing to a capacity of 3670 MW [9-10]. This capacity includes the Sakaka solar and Domat Al Jandal wind projects. Concurrently, the Public Investment Fund of Saudi Arabia has unveiled ambitious plans for the Sudair Solar PV project, poised to become the largest solar plant in the nation. With an estimated investment value of SAR 3.4 billion and a capacity of 1,500 MW, the Sudair Solar PV project is projected to provide power to 185,000 households while mitigating over 2.9 million tons of emissions annually. Nonetheless, integrating solar PV systems into the grid presents several challenges, given that the existing grid infrastructure was not initially designed to accommodate high levels of PV penetration [11]. Solar PV generation is intermittent, reliant on weather conditions, and unavailable during nighttime hours. Consequently, a substantial portion of the power injected into the grid from PV sources exhibits intermittent behavior. Moreover, unlike conventional energy sources, the output from solar PV systems cannot be easily adjusted to match fluctuating load demands. These intricacies in energy generation can impact the operation and stability of PV-connected grids. Studies in [12] and [13] indicate that numerous catastrophic failures and blackouts in the past three decades have been linked to voltage instability. Consequently, voltage instability has become a significant concern for power systems integrating intermittent PV generation [14], [15]. Voltage stability in a power system refers to its ability to maintain voltage levels within acceptable limits across the network during normal operations and disturbances [16]. As solar PV systems become increasingly integrated into grids, evaluating the power grid's voltage stability and promptly implementing corrective measures to prevent potential system failures is essential. Several research has delved into the effects of different levels of PV penetration on system voltage stability [17], [18], [19]. For example, findings from [17] indicate that the impact of PV integration on grid voltage stability can vary, with outcomes ranging from adverse to beneficial, contingent upon factors like PV installation locations and penetration levels. In [18], the PV curve method was utilized to assess the influence of varying PV penetration levels on the voltage stability of distribution networks. Findings indicate that higher PV penetration levels can enhance the grid's loading margin and reduce grid losses by up to 30%. Additionally, research in [19] demonstrates that changes in PV penetration levels exhibit a quadratic relationship with voltage fluctuations in extensive transmission systems for specific load demands. Conversely, [20] suggests that in low-voltage distribution networks, intermittent PV generation may lead to voltage fluctuations and short-term instability, particularly during fault conditions. Sreekumar et al. [21] examined the effects of grid-connected distributed PV systems on distribution networks, specifically focusing on power

losses and voltage drops caused by PV systems. These effects are more pronounced when large-scale PV installations near lightly loaded, long distribution feeders. Furthermore, [22] illustrates that PV energy sources can enhance a power grid's voltage stability if the associated inverters provide reactive power support. Simulation outcomes in [23-24] underscore the significance of voltage control capabilities in PV energy systems, as systems lacking such capabilities may trigger voltage fluctuations at the point of common coupling (PCC), particularly during abrupt changes in solar irradiation. This effect is particularly pronounced with high levels of PV penetration. Power flow analyses indicate increased PV generation directly undermines voltage stability [25, 26-29]. PV systems are vulnerable to risks stemming from weather conditions, leading to sudden decreases in generation. One proposed solution involves deploying emergency battery energy storage to reinforce grid resilience under such circumstances [30]. Furthermore, the limited reactive power regulation capability of PV systems is acknowledged as a significant concern. While employing large-capacity inverters and reactive power resources for enhanced flexibility is feasible, it entails substantial costs [30, 31]. Studies conducted on a modified IEEE 13-bus test system have indicated that PV penetration below 40% does not notably affect the system [32]. Additionally, it has been demonstrated that PV can improve voltage stability on a smaller scale by reducing long-distance power transfers [33]. Moreover, distributed PV generators have less impact on voltage stability than centralized PV farms [31]. Further research focusing on penetration levels between 0-16% indicates a trend of decreasing voltage magnitude with increasing penetration, a trend expected to persist beyond the 16% threshold [32]. It has also been demonstrated that PV can enhance voltage stability on a smaller scale by reducing long-distance power transfers [33]. Furthermore, dispersed PV generators have a lesser impact on voltage stability than centralized PV farms [31]. Additional research focusing on penetration levels between 0-16% reveals a trend of decreasing voltage magnitude with increasing penetration, a trend expected to persist beyond the 16% threshold [32]. Large-scale PV systems have demonstrated the capability to generate reactive power [34]. Nevertheless, their reactive power generation is usually constrained by grid codes, frequently operating near unity power factor (typically around 0.95 lead-lag power factor). Nonetheless, the size and positioning of large PV generators can significantly impact power system voltage stability, especially as PV penetration reaches a significant percentage of total installed power. Hence, this research aims to assess the effect of extensive solar adoption on the voltage stability of the Saudi distribution system. Both static power flow analysis and time-domain simulation techniques were employed to examine the implications of PV integration during peak demand periods. The following research questions guide the study:

- Does the high level of PV integration cause voltage instability in the Saudi distribution network?
- How does PV systems penetration impact power flow losses within the Saudi distribution network?
- What is the maximum permissible level of solar PV penetration?

This research paper contributes in the following ways:

- Developing a model for the electrical distribution network in Saudi Arabia incorporating a grid-connected PV farm.
- The model he developed is then utilized to assess how the PV farm affects the voltage stability of the electrical distribution network.
- To design an advanced voltage controller with PSCAD and PSSE software to stabilize the voltage.
- To determine the maximum PV penetration level.

This paper is organized as follows: Section 2 contains a qualitative analysis of the impact of the PV on voltage stability. Section 3 describes the effect on the active and reactive power margin. The system description and simulation results are presented and discussed in Sections 4 and 5, and the study is concluded in Section 6.

2. Analysis of Pv's Impact on Voltage Stability (Qualitative)

The displacement of synchronous generators with PV affects voltage stability due to PV generation's distinctive voltage and reactive power control characteristics. Equations derived from a simple radial system, as illustrated in Fig. 1, are utilized to investigate the impact of PV on voltage stability.

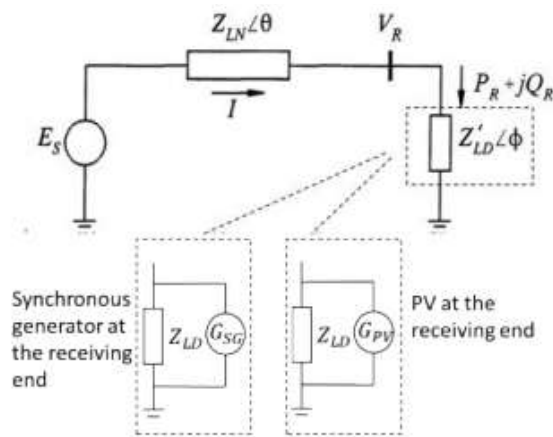


Fig 1. A simple radial system diagram.

For a simple radial system [35], the receiving end voltage is shown in Equation (1)

$$V_R = Z_{LD}I = \frac{1}{\sqrt{F}} \frac{Z_{LD}}{Z_{LN}} E_S \quad (1)$$

The receiving end power is shown in Equation (2)

$$P_R = V_R I \cos \phi = \frac{Z_{LD}}{F} \left(\frac{E_S}{Z_{LN}} \right) \cos \phi \quad (2)$$

Because of the limited converter current capacity in PV systems, their reactive power capability tends to be smaller than synchronous generators, especially when the real power output of the PV system approaches its rated value. Consequently, in scenarios where there is a higher penetration of PV at the receiving end and the reactive power limit of the PV system is reached, there could be an increase in reactive power demand as the load rises. This results in a further lagging power factor of the equivalent load impedance ($\cos \phi$), which, as per equations (1) and (2), leads to a reduced voltage stability margin. For accurate load flow simulations, it's imperative to represent the equivalent PV generator as a standard generator rather than a negative load. Solar PV inverters can autonomously regulate both active and reactive power, as illustrated in Figure 2, which showcases the capability curve of the solar PV system [36]. As illustrated in Figure 2, The reactive power capability is significant at low active power levels, corresponding to lighter loading conditions. Furthermore, as depicted in Figure 3, solar PV systems mainly operate below their rated active power for the majority of the day, showcasing considerable reactive power capability throughout the operational timeframe. Therefore, it is crucial to investigate long-term voltage stability phenomena under both full-load and partial-load conditions.

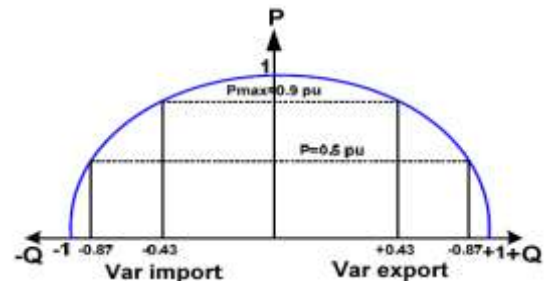


Fig. 2. Solar-PV system capability curve.

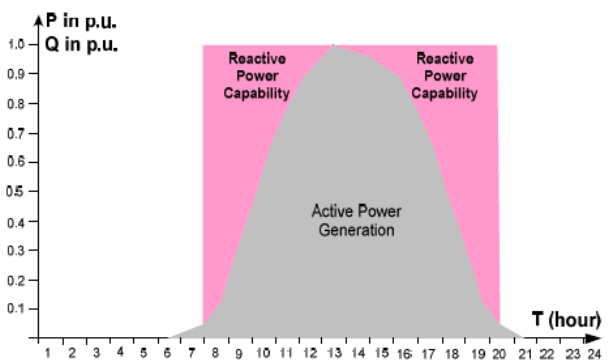


Fig. 3. Typical solar-PV system generation curve.

3. Impact on the active and reactive power margin

a. PV System Model in Power Flow

PV power generation comprise of PV arrays, controllers, inverters, and associated components. When modeling a PV power generator to analyze directional effects, focusing only on steady-state results suffices without examining the dynamic characteristics of the control system tuning process. The configuration and attributes of the transformer dictate the suitable sequence for electrical power output. Figure 4 states a high-penetration PV system on the grid [14].

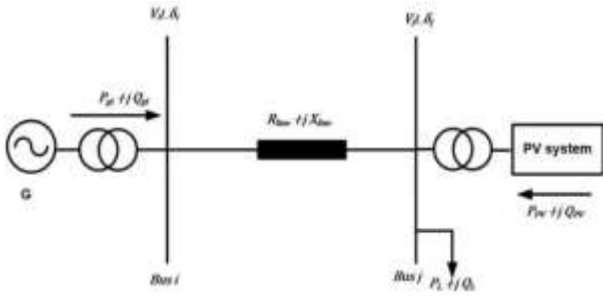


Fig. 4. High-penetration PV system connected to the Power system.

The equality constraints are active/reactive power flow equations as [14]:

$$P_{PVj} = P_{Lj} + V_j \cdot \sum_{i=1 \rightarrow n_{bus}} V_i \cdot Y_{ij} \cdot \cos(\theta_{ij} + \delta_i - \delta_j) \quad (4)$$

$$Q_{PVj} = Q_{Lj} + V_j \cdot \sum_{i=1 \rightarrow n_{bus}} V_i \cdot Y_{ij} \cdot \sin(\theta_{ij} + \delta_i - \delta_j) \quad (5)$$

$$i = 1, \dots, n_{bus} \quad (6)$$

where P_{PVj} and Q_{PVj} are generated active and reactive powers of PV system bus j , P_{Lj} , and Q_{Lj} are load active and reactive powers bus j , V_i and V_j are the magnitude of the voltage at buses i , and j , Y_{ij} , and θ_{ij} are the magnitude of admittance magnitude and the angle of the line between bus i and j . The active and reactive powers of the PV system P_{PVj} and Q_{PVj} depend on the weather conditions (irradiation and temperature). The actual power output P_{PV} extracted from the PV system can be written as:

$$P_{PV} = \sum_{n=1 \rightarrow n_{PV}} P_{gPV} \quad (7)$$

$$P_{PV} \propto G \quad (8)$$

where G is the irradiation value (W/m^2). The standard value of irradiation of PV systems is $1000 W/m^2$. The output power of PV at the different values of irradiation can be calculated by:

$$P_{PV} = P_{PVr} \cdot (G/1000) \quad (9)$$

where P_{PVr} is the rated output power of the PV system at the irradiation value of $1000 W/m^2$.

The output reactive power Q_{PV} can be calculated by:

$$Q_{PV} = m P_{PV} \quad (10)$$

where m depends on the PV system's power factor (pf) and can be adjusted using pf of the PV system, $m = 0.44$ for pf = 0.9 .

4. PV/ QV curves analysis

The PV/QV analysis is designed to study steady-state loanability limits related to the voltage stability of radial systems and large mesh networks. The voltage variation concerning active and reactive power variations is evaluated using power flow techniques. These two techniques do not provide solutions to stability issues. They are tools used to analyze steady-state voltage stability issues associated with power systems.

The PV curve is a parametric study implying AC load flow analysis that systematically monitors the changes in power flow variables in a set. It is a powerful technique that determines active power transfer limits concerning voltage. The low transfer limit capability is related to where voltage reaches the low value at the knee point. Eventually, each bus has its knee points, where the buses devoted to the transfer path typically demonstrate greater predictability at a knee point, as shown in Figure 5. Thus, monitoring what happens to the bus voltage as a result. The distance between the operating and maximum loading points is known as the loading margin, real power margin, or voltage stability margin [37-38]. The drawback of this technique is that power flow should be done on many buses, which takes time because there is no prior knowledge about the critical buses. Hence, there is no helpful information about the causes of voltage instability. Besides, at different power factors, the maximum power and critical voltage are higher at higher pf.

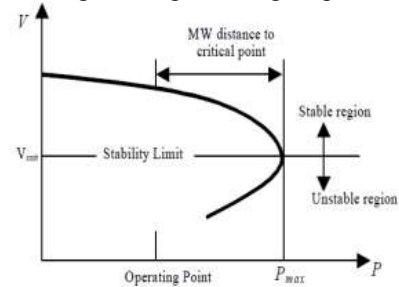


Fig. 5. Typical PV curve.

In the PSSE, the PV curve is created by choosing two subsystems. One of them is a source, while the other is a sink. The power flows from the source to the sink bus. AC power flow simulation increments the power transfer between the subsystems in a predefined step size by monitoring the bus voltage, generator output, and the network. The PV curve can be sketched when the bus voltages are mapped as a function of the incremental power transfer. The QV curve is one of the most popular ways to explore voltage instability challenges in a power system during the post-transient period. QV curves determine the reactive power injection or absorbing for various scheduled voltages required at a bus to vary the bus voltage to the required value [39-40]. The curve is sketched starting with existing reactive loading at the

particular bus. Then, the voltage is evaluated for a power flow as the reactive load increases in predefined steps. The voltage collapse point is determined as the system-imposed low convergence difficulties while the process is continued. Figure 6 shows the typical QV curve obtained that is stable at normal loading and unstable at higher loading. The minimum reactive power requirement for the stable operation can be determined at the bottom of the curve, hence representing the voltage stability limit. The size and type of compensation needed to provide voltage stability are obtained by examining the curve. Thus, the capacitor bank characteristics are drawn over the system QV curve. Utilities widely use the vicinity to voltage collapse using QV. In addition, the voltage stability of the system is monitored to take appropriate control action.

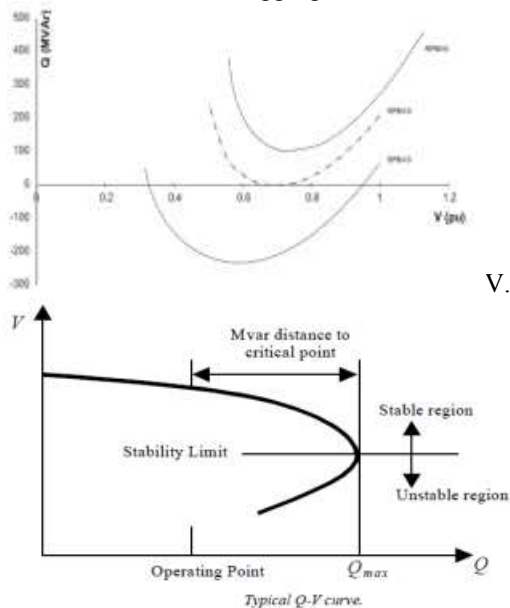


Fig. 6. Typical QV curve.

5. System description

The single-line diagram of the proposed 300 MW solar power plant's transmission grid is depicted in Figure 7-a. This network encompasses 22 MV bus bars. A 300 MW PV power plant model has been meticulously constructed and interconnected with the distribution power grid at bus 1 as shown in Fig. 7-b. This plant consists of 150 PV arrays, each with a rating of 2 MWp. These arrays are linked to the grid via a three-phase inverter and a step-up transformer. The modular inverter, comprising multiple parallel units, carries a rating of 2 MW. Each transformer boasts a power capacity of 2 MVA, with a rated frequency of 60 Hz and a voltage ratio of 0.4/22 kV. Simulations utilizing PSCAD software have been executed to capture the active and reactive power outputs delivered to the grid and the voltage at each point for the integrated generators [26-27]. Table 1 showcases the V_{dc} and current controller values [28], while Table 2 outlines the PV array parameters [29], encompassing a fill factor of 0.73, indicative of solar PV panel efficiency.

Table 1. V_{dc} and current controller values.

Parameters of the controller	Value
Nominal power P_{nom}	2 MW
Nominal frequency	50 Hz
Initial DC voltage	700 V
Nominal DC voltage U_{dc}	700 V
Rated power P_{nom}	20 MW
V_{dc} regulator gains K_p and K_i	7 and 800
The current regulator gains K_p and K_i	0.3 and 20
Choke impedance	1 m Ω , 250 μ H
Transformer leakage impedance $R_x f_o, L_{xf} / P_{nom}$	0.002, 0.06

Table 2. PV array parameters.

PV array parameters	Value
Open circuit voltage V_{oc}	64 V
Short-circuit current I_{sc}	5.87 A

MPPT voltage V_{mp}	54.7 V
MPPT current I_{mp}	5.49 A
Number of parallel modules N_p	445
Number of series modules N_s	15

6. Simulation results and discussions

6.1 Static voltage and loss analysis comparisons

The system is examined with and without consideration of solar penetration. A load flow calculation and active and reactive power losses were performed. Also, The study observed the maximum permissible PV penetration levels without infringing statutory limits under both no-load conditions (representing the worst-case scenario) and peak load conditions.

Voltage profiles of both cases have been compared in the following table. The voltages are improved when the local power plant is connected. The voltage profile of the Saudi Arabia distribution network before and after injecting a local generation source is measured, as seen in the attached table. The voltages remained within the acceptable statutory limits outlined in the Saudi grid code. Grid code voltage limits were upheld until solar integration reached a steady state value of 100% (300 MW). Moreover, the voltage profile of the Saudi Arabia distribution network is enhanced following the injection of an additional generation source, as depicted in the Table 3. Moreover, the voltage profile of the source bus is also enhanced from 0.9569 pu to 0.9788 pu. The simulation results indicate that the system is stable.

The system losses in MW (real power) and MVAR (reactive power) have been observed in Tables 4 and 5. These tables show a reduction in power losses as solar PV penetration increases from 0 MW to its nominal value, especially in the lines close to the PV bus, compared with the losses of the normal system. The same tables show that the real and reactive power losses are not decreased when injecting solar power into some transmission lines.

Thus, the power generated by the PV plants must traverse considerable distances to reach the network loads, resulting in increased losses within the system. Additionally, the output power of the PV plants is constrained by the availability of solar irradiance. Consequently, the placement of large-scale PV plants notably impacts voltage stability.

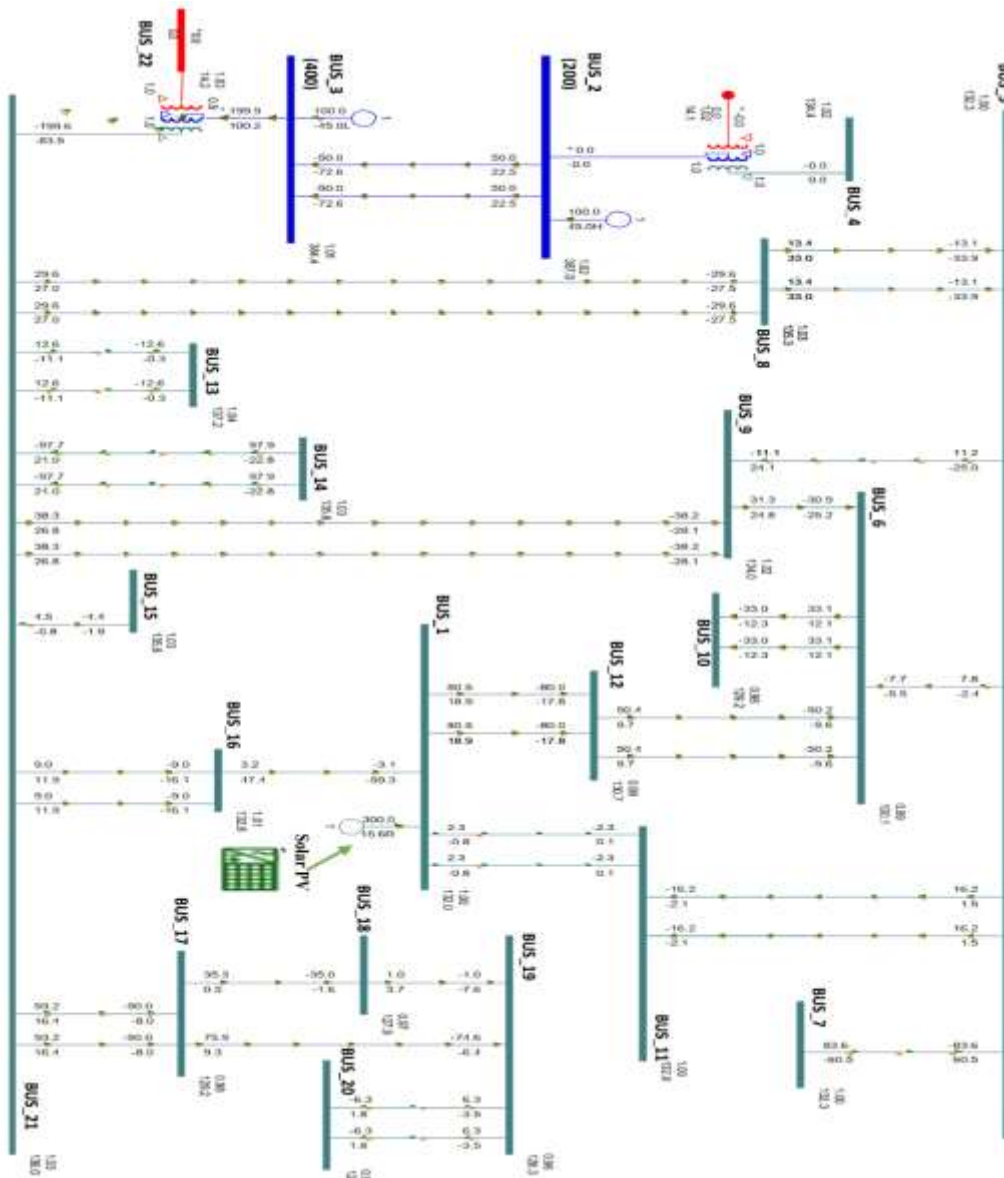


Figure 7-a. Saudi Arabia's transmission network with 300 MW solar PV integration is under study.

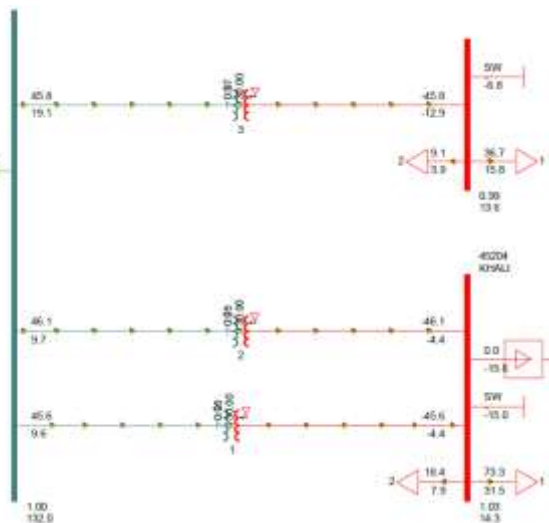


Figure 7-b. Saudi Arabia distribution network under study with 300 MW solar PV integration.

Table 3. Comparison of Voltages in Reduced Base Case

Bus #	Voltage (pu) –without Solar farm	Voltage (PU) –with Solar farm
Bus 1	1.000	1.0000
Bus 2	1.007	1.0070
Bus 3	1.0095	1.0054
Bus4	0.9694	1.0054
Bus_5	0.9621	0.9953
Bus_6	0.9723	0.9884
Bus_7	0.98	1.0005
Bus_8	0.9788	1.0111
Bus_9	0.9569	0.9788
Bus_10	0.9577	0.9569
Bus_11	1.0394	0.9577
Bus_12	1.0148	1.0394
Bus_13	0.993	1.0178
Bus_14	0.969	1.0072
Bus_15	1.03	0.9690
Bus_16	0.9883	1.0300
Bus_17	1.0264	1.0159
Bus_18	1.000	1.0260
Bus_19	1.0286	1.0000
Bus_20	1.03	1.0286
Bus_21	0.9843	1.0070
Bus_22	0.9751	1.0274
Bus_23	0.9831	0.9799
Bus_24	1.0392	0.9751
Bus_25	0.9752	0.9831
Bus_26	1.0291	0.9578
Bus_27	1.024	1.0392
Bus_28	0.9664	0.9752
Bus_29	0.9679	1.0287
Bus_30	0.9828	1.0240
Bus_31	0.9925	1.0197
Bus_32	0.9656	1.0270
Bus_33	0.9946	1.0270
Bus_34	1.0075	1.0270
Bus_35	0.9887	1.0100
Bus_36	1.0139	1.0100
Bus_37	1.0099	1.0100

Table 4. Comparison of active power losses in the reduced base case.

From Bus	To Bus	MW Losses – Without Solar farm	MW Losses – With Solar farm
Bus_1	Bus_2	0	0
Bus_1	Bus_2	0	0
Bus_3	Bus_39	-0.8	0
Bus_3	Bus_4	0.6	0.1
Bus_3	Bus_12	0.3	0.1
Bus_3	Bus_13	1.4	0
Bus_3	Bus_13	1.4	0
Bus_3	Bus_17	0.2	0.2
Bus_3	Bus_17	0.2	0.2
Bus_4	Bus_5	0.1	0.1
Bus_4	Bus_5	0.1	0.1
Bus_4	Bus_6	0	0.2
Bus_4	Bus_6	0	0.2
Bus_4	Bus_12	1.6	0.4
Bus_6	Bus_7	0.3	0.4
Bus_6	Bus_7	0.3	0.4
Bus_7	Bus_13	0.9	0
Bus_7	Bus_13	0.9	0
Bus_7	Bus_16	0	0
Bus_8	Bus_9	1.3	1.3
Bus_8	Bus_14	0.3	0.3
Bus_8	Bus_15	3.2	3.2
Bus_8	Bus_15	3.2	3.2
Bus_9	Bus_10	0	0
Bus_9	Bus_10	0	0
Bus_9	Bus_14	0	0
Bus_11	Bus_15	0	0
Bus_11	Bus_15	0	0
Bus_12	Bus_15	0.1	0.1
Bus_12	Bus_15	0.1	0.1
Bus_15	Bus_16	0.4	0.1
Bus_15	Bus_16	0.4	0.1
Bus_15	Bus_17	0	0
Bus_15	Bus_17	0	0
Bus_15	Bus_19	0.1	0.1
Bus_15	Bus_40	0.2	0.2
Bus_15	Bus_40	0.2	0.2

Table 5. Comparison of reactive power losses in the reduced base case

From Bus	To Bus	Reactive power losses Without Solar farm	Reactive power losses – With Solar farm
Bus_1	Bus_2	-49	-49
Bus_1	Bus_2	-49	-49
Bus_3	Bus_39	0	0
Bus_3	Bus_4	-6.1	0.2
Bus_3	Bus_12	37	-1
Bus_3	Bus_13	3.9	-0.5
Bus_3	Bus_13	3.9	-0.5
Bus_3	Bus_17	-1.1	-1.1
Bus_3	Bus_17	-1.1	-1.1
Bus_4	Bus_5	-0.2	-0.2
Bus_4	Bus_5	-0.2	-0.2
Bus_4	Bus_6	-0.2	0.1
Bus_4	Bus_6	-0.2	0.1
Bus_4	Bus_12	3.4	-0.8
Bus_6	Bus_7	0.3	1.1
Bus_6	Bus_7	0.3	1.1
Bus_7	Bus_13	2.6	-0.6
Bus_7	Bus_13	2.6	-0.6
Bus_7	Bus_16	-10.9	-12.3
Bus_8	Bus_9	2.9	2.9
Bus_8	Bus_14	-1.1	-1.1
Bus_8	Bus_15	8.4	8.4
Bus_8	Bus_15	8.4	8.4
Bus_9	Bus_10	-1.7	-1.7
Bus_9	Bus_10	-1.7	-1.7
Bus_9	Bus_14	-3.9	-3.9
Bus_11	Bus_15	-11.4	-11.4
Bus_11	Bus_15	-11.4	-11.4
Bus_12	Bus_15	-1.2	-1.4
Bus_12	Bus_15	-1.2	-1.4
Bus_15	Bus_16	-2	-4.4
Bus_15	Bus_16	-2	-4.4
Bus_15	Bus_17	-0.7	-0.5
Bus_15	Bus_17	-0.7	-0.5
Bus_15	Bus_19	-2.7	-2.7
Bus_15	Bus_40	-1.8	-1.8
Bus_15	Bus_40	-1.8	-1.8

6.2 PV analysis comparisons with solar PV farm

Figure 8 illustrates the V-P curves for the load nodes of the Saudi Arabia distribution network node test system. These curves were derived by calculating the positive sequence components of voltage based on power variations. Upon examining the PV curve for the solar PV generation bus within the PSS/E, it becomes apparent that there is a linear relationship between active power and voltage within the specified range of 0.95 to 1.05 p.u at generator-controlled buses. However, an increase in active power from solar PV generation buses is observed to lead to a dip in voltages for certain distribution buses. This underscores the significance of the operating point. The analysis of this curve proves crucial in comprehending the system's voltage stability characteristics, necessitating the development of strategies to mitigate potential issues. The operating point is vital because voltage instability issues beyond 300 MW are observed. In the rising photovoltaic generation margin, the bifurcation voltage diagram at distribution buses is shown in the same figure. As PV power injected increases to approximately 200 MW, the voltage also rises, predominantly in the first half of the curve. This trend is driven by the feeder's reduction in active power injection into the power system. Subsequently, in the second half of the curve, voltage tends to decrease, often exhibiting nose curves, as the feeder returns to its regular power flow. PV farms supply power to the grid and meet neighborhood load demands. The network's maximum penetration of photovoltaic farms can sustain up to 462 MW.

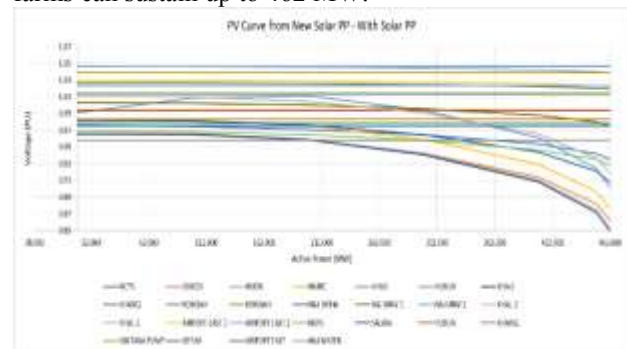


Fig. 8. The PV curves.

6.3 QV analysis comparisons without solar PV farm

The Q-V analysis curve depicts the relationship between reactive power (Q) and voltage (V) at a specific bus or generator in a power system. This graphical representation is pivotal for assessing the reactive power capabilities of a device and understanding its impact on voltage stability. In Figure 9, it is evident that voltage control has played a significant role in enhancing the penetration level of photovoltaic power (PVP) at integration points by regulating the reactive power injected at these buses. This voltage control method has effectively maintained the voltage profile at the terminals of PVP power stations and

surrounding substations, as depicted in the figures. Furthermore, the voltage stability of a specific substation within the grid is directly impacted by the equivalent impedance of the electric network at that location. A higher equivalent impedance results in greater voltage sensitivity and restricts the real power that can be injected at that point. The curve also typically exhibits a positive slope from -180 MVAR to 85 MVAR, indicating an increase in reactive power with an increase in voltage, or a negative slope, indicating a decrease in reactive power with a rise in voltage. Critical points such as the maximum reactive power (Q_{max}) and the minimum voltage (V_{min}) highlight operational limits. According to the U-Q curve, we can obtain the maximum reactive power that needs to be extracted from the solar PV bus to reach a minimum voltage level of 0.90 p.u. (a maximum deviation of +/- 10 % is considered). The Q-V curve assists in developing control strategies for generators, pinpointing issues related to voltage stability, and optimizing the flow of reactive power within the system. A comprehensive analysis of this curve provides valuable insights into the dynamic behavior of the power system, allowing for the evaluation of the impact of changing conditions on reactive power. This, in turn, facilitates formulating strategies to sustain stable and efficient system operation.

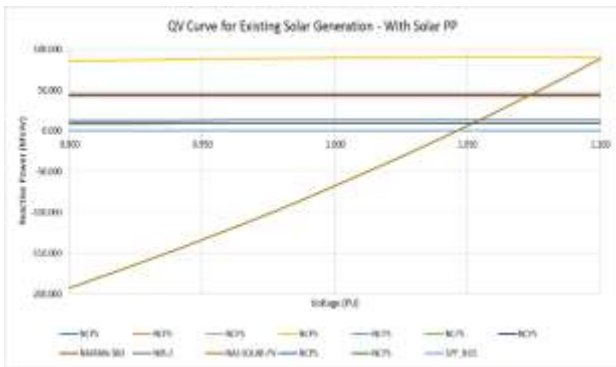


Fig. 9. The QV curve.

6.4 Base case scenario on the reduced network – with and without solar farm.

Extensive dynamic voltage stability simulation studies are conducted using the PSCAD power system analysis software. These studies analyzed the impact of PV system behavior on power system steady-state stability, considering network terminal voltage and generator output of electrically active and reactive power. The analysis encompassed four voltage levels: 380 kV, 132 kV, 33 kV, and 13.8 kV, focusing on normal operating conditions.

No variation is observed in the system's state variable under a normal operating scenario. The source buses deliver 100 MW of power at 380 kV (Fig. 10-a) and 600 MW at 132 kV (Fig. 12-a) under normal cases without solar PV farms. This generation of active power will be less (95 MW at 380 kV (Fig. 10-b) and 450 MW at 132 kV (Fig. 12-b)) in the case when integrating the solar PV farm to satisfy the demand of the local network without any stability issue. In case of no PV power, the swing bus

delivers 45 MVAR at 380 kV (Fig. 11-a) and -37 Mvar at 132 kV (Fig. 13-a) from the two SG power plants. This total reactive power generated by the three power plants is decreased in the case of PV farm integration (see Figs. 11-b and 13-b) due to the control mode available by the solar PV bus.

As this scenario reflects the steady state stability, and as the PV farm works in voltage regulation mode, we can see from Figures 14 and 17 that the voltage variations at 33 kV and 13.8 kV are stable. It can also be observed that the generation is stable without any oscillation in the output. All active power flow (Fig. 15) of the load buses in the Saudi distribution network is stable, and the power consumption under normal cases is to satisfy the demand without any power quality issues or oscillation. All reactive power flows (Fig. 16) at the load buses in the Saudi distribution network are stable, and consumption of reactive power under normal cases is to satisfy the demand without any power quality issues and oscillation.

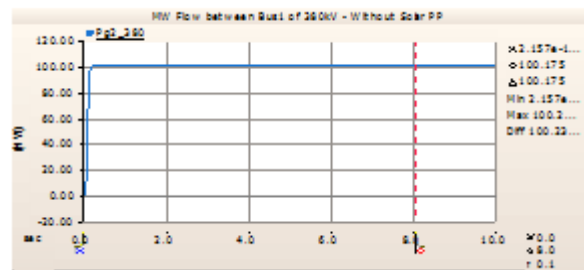


Fig. 10-a. Active power generation at 380 kV under normal conditions without solar PV farms.

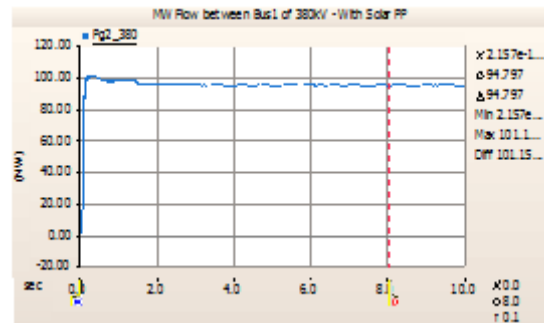


Fig. 10-b. Active power generation at 380 kV under normal conditions with solar PV farms.

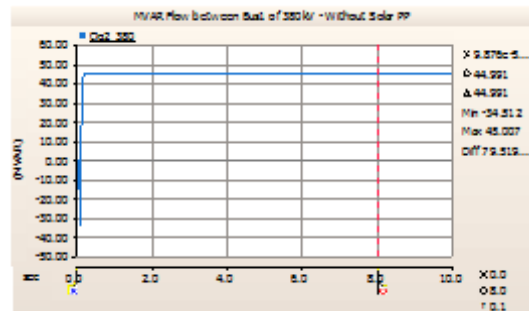


Figure 11-a. Reactive power generation at 380 kV under normal conditions without a solar PV farm.

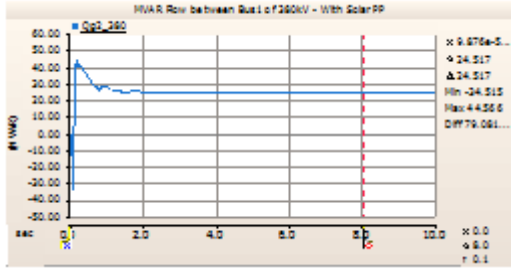


Fig. 11-b. Reactive power generation at 380 kV under normal conditions with a solar PV farm.

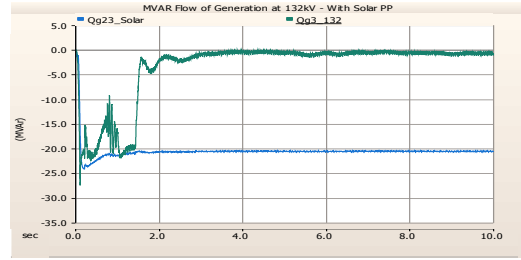


Fig. 13-b. Reactive power generation at 132 kV under normal case with Solar PV farm.

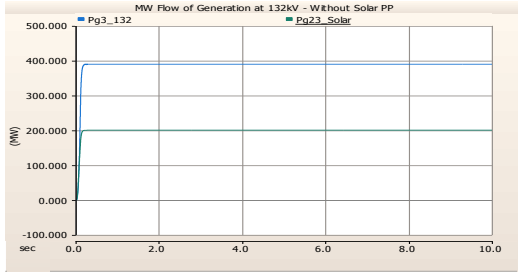


Fig. 12-a. Active power generation at 132 kV under normal conditions without solar PV farms.

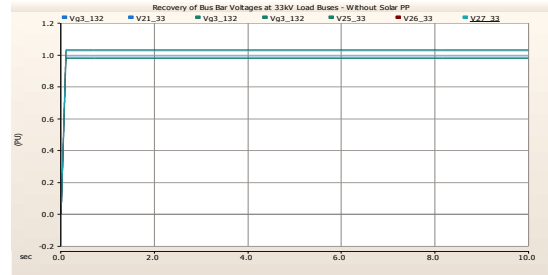


Figure 14-a. Voltage load variation at 33 kV under normal case without solar PV farm.

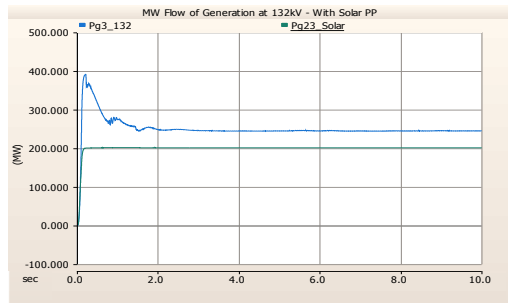


Fig. 12-b. Active power generation at 132 kV under normal conditions with solar PV farms.

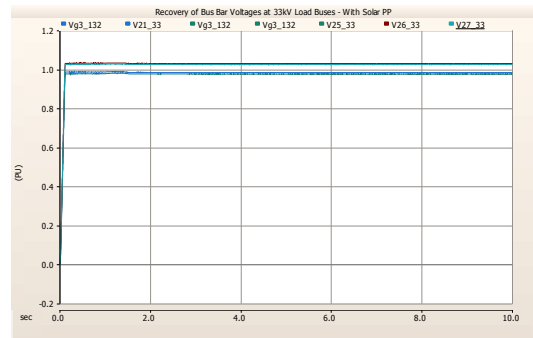


Figure 14-b. Voltage load variation at 33 kV under normal case with solar PV farm.

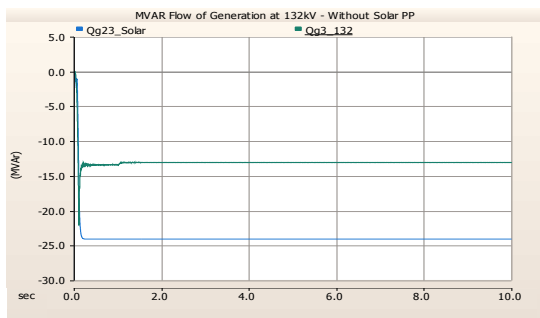


Fig. 13-a. Reactive power generation at 132 kV under normal case without Solar PV farm.

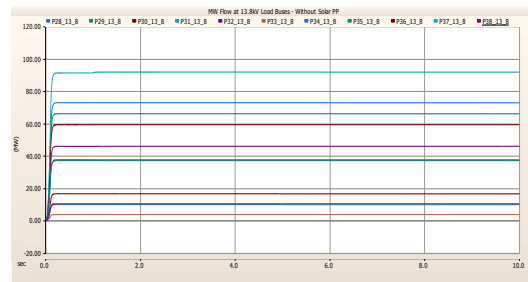


Figure 15-a. Active power load at 13.8 kV under normal case without solar PV farm.

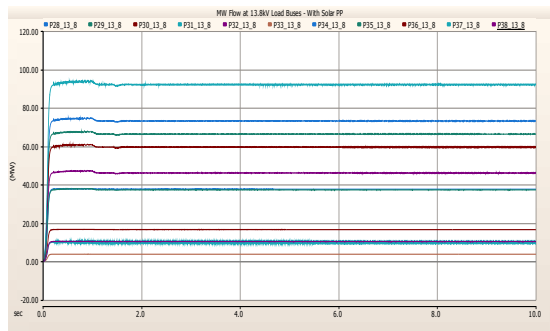


Figure 15-b. Active power load at 13.8 kV under normal case with solar PV farm.

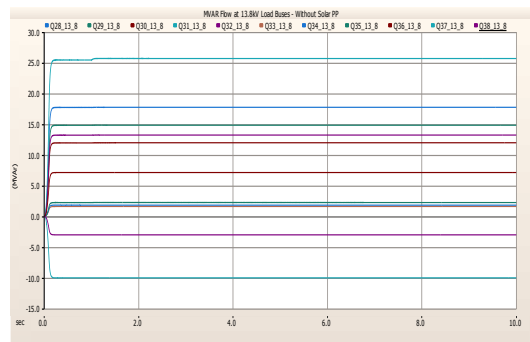


Figure 16-a. The reactive power load at 13.8 kV under normal conditions without a solar PV farm.

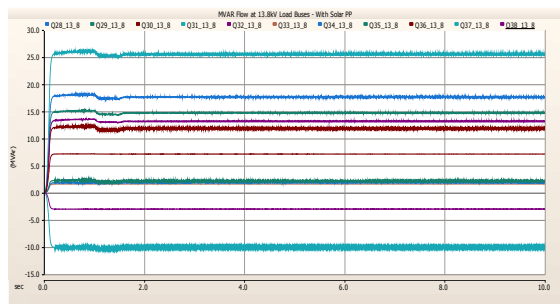


Figure 16-b. The reactive power load at 13.8 kV under normal conditions with a solar PV farm.

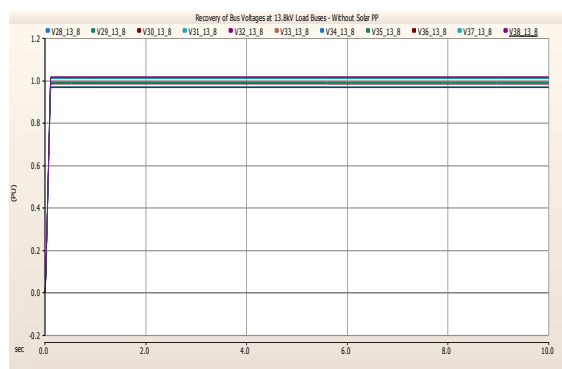


Figure 17-a. Voltage load variation at 13.8 kV under normal case without solar PV farm.

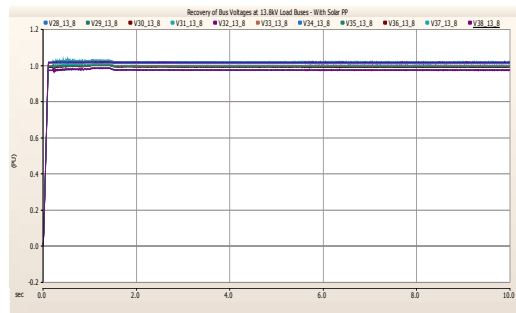


Figure 17-b. Voltage load variation at 13.8 kV under normal case with Solar PV farm.

7. Conclusion

The performance of the Saudi distribution grid under high levels of photovoltaic power generation is demonstrated through computational simulations using the PSCAD and PSSE software packages. Assessments of the impact of increased PV penetrations on the Saudi distribution power system's capacity were conducted using various methodologies, including the Newton-Raphson load flow method, PV and QV method, and time domain simulation in the base case scenario. Considering constraints on transmission line capacity, simulation results confirmed that the proposed PV farm station's maximum allowable generation did not exceed 462 MW. The network's static and dynamic voltage stability concerning the integration of large-scale photovoltaic generation was examined. To this end, a Saudi electrical distribution network model with 300 MW solar PV penetration was developed. This model was utilized to investigate the effects of voltage regulation and power flow analysis on the electrical distribution network. Additionally, a voltage controller was implemented to regulate voltage drop at the point of common coupling (PCC) and mitigate reverse power flow issues under worst-case scenarios of maximum power output from a PV bus. Simulation results highlighted that integrating a PV farm into the distribution network improves the voltage profile of the power system and reduces both active and reactive power losses.

References

- [1]. Kabir E. et al. Solar energy: Potential and future prospects. *Renewable and Sustainable Energy Reviews*. Volume 82, Part 1, February 2018, Pages 894-900. <https://doi.org/10.1016/j.rser.2017.09.094>
- [2]. Devabhaktuni V. et al. Solar energy: Trends and enabling technologies. *Renewable and Sustainable Energy Reviews*. Volume 19, March 2013, Pages 555-564. <https://doi.org/10.1016/j.rser.2012.11.024>
- [3]. Tyagi V. et al. Progress in solar PV technology: Research and achievement. *Renewable and Sustainable Energy Reviews*, 2013, vol. 20, issue C, 443-461. [10.1016/j.rser.2012.09.028](https://doi.org/10.1016/j.rser.2012.09.028)

- [4]. "Renewables 2023: Global Status Report," Renewable Energy Policy Network for the 21st Century, 2023. [Online]. <https://www.ren21.net/reports/ren21-reports/>
- [5]. US Energy Information Administration. 2021. "Country Analysis Executive Summary: Saudi Arabia". https://www.eia.gov/international/anal-864-ysis/country/SAU_865
- [6]. Saudi F. Al Harbi and D. Csala, "Saudi Arabia's Electricity: Energy Supply and Demand Future Challenges". 1st Global Power, 866 Energy and Communication Conference (GPECOM), Nevsehir, Turkey, 2019, pp. 467-472, doi: [10.1109/GPECOM.2019.8778554](https://doi.org/10.1109/GPECOM.2019.8778554)
- [7]. Al Ghamdi, A. "Saudi Arabia Energy Report", 15 December 2020. Available online: <https://www.kapsarc.org/file-download.php?i=72975>
- [8]. Saudi Press Agency; Al-Sultan, K.B.S. "Chairman of KACARE: Saudi Arabia Aims to Adopt Electricity Production Using Renewable Energy by 50% in 2030," 19 January 2021. Available online: <https://www.spa.gov.sa/2181891>
- [9]. Gulf Research Center. Saudi Arabia Renewable Energy Industry Outlook. Gulf Research Center Report 2022. Available online: <https://www.caschi.ch/wp-content/uploads/Saudi-Arabia-Renewable-Energy-Industry-Outlook.pdf>
- [10]. Saudi Aramco, Bond Prospectus, 16 November 2020, p. 45. Available online: <https://www.aramco.com/en/Investors/Investor-tools/Bond-information>
- [11]. Suampun W. Voltage stability analysis of grid-connected photovoltaic power systems using CPFLOW Procedia Computer Science. Volume 86, 2016, Pages 301-304. <https://doi.org/10.1016/j.procs.2016.05.082>
- [12]. Nwaigwe K. *et al.* An overview of solar power (PV systems) integration into electricity grids. Materials Science for Energy Technologies. Volume 2, Issue 3, December 2019, Pages 629-633. <https://doi.org/10.1016/j.mset.2019.07.002>
- [13]. Gusman L. *et al.* Design for reliability of multifunctional PV inverters used in industrial power factor regulation. International Journal of Electrical Power & Energy Systems. Volume 119, July 2020, 105932. <https://doi.org/10.1016/j.ijepes.2020.105932>
- [14]. Azad, S.; Amiri, M.M.; Heris, M.N.; Mosallanejad, A.; Ameli, M.T. A Novel Analytical Approach for Optimal Placement and Sizing of Distributed Generations in Radial Electrical Energy Distribution Systems. *Sustainability* **2021**, *13*, 10224. <https://doi.org/10.3390/su131810224>
- [15]. Modarresi, Javad & Gholipour, Eskandar & Khodabakhshian, Amin, 2016. "A comprehensive review of the voltage stability indices," *Renewable and Sustainable Energy Reviews*, Elsevier, vol. 63(C), pages 1-12. [10.1016/j.rser.2016.05.010](https://doi.org/10.1016/j.rser.2016.05.010)
- [16]. Adetokun B.B. *et al.* Voltage stability assessment and enhancement of power grid with increasing wind energy penetration. International Journal of Electrical Power & Energy Systems. Volume 120, September 2020, 105988. <https://doi.org/10.1016/j.ijepes.2020.105988>
- [17]. Munkhchuluun E. *et al.* Long-term voltage stability with large-scale solar-photovoltaic (PV) generation. International Journal of Electrical Power & Energy Systems. Volume 117, May 2020, 105663. <https://doi.org/10.1016/j.ijepes.2019.105663>
- [18]. T. Aziz, S. Dahal, N. Mithulananthan, and T. K. Saha, "Impact of widespread penetrations of renewable generation on distribution system stability," in International Conference on Electrical & Computer Engineering (ICECE 2010). IEEE, 2010, pp. 338-341.
- [19]. Hossain J. *et al.* Robust control for grid voltage stability: high penetration of renewable energy. Springer; 2014th edition (July 28, 2014).
- [20]. Xu Y. *et al.* Assessing short-term voltage stability of electric power systems by a hierarchical intelligent system. *IEEE Transactions on Neural Networks and Learning Systems* (Volume: 27, Issue: 8, August 2016). [10.1109/TNNLS.2015.2441706](https://doi.org/10.1109/TNNLS.2015.2441706)
- [21]. Sree Kumar, S.; Savier, J.S. Investigative scheme to assess ultimate penetration level of grid connected solar photovoltaic systems in distribution network. International Transactions on Electrical Energy System. *Special Issue: Control and power in renewable energy systems*. Volume 31, Issue 10. **2021**, e12647. <https://doi.org/10.1002/2050-7038.12647>
- [22]. Almeida A.B. *et al.* Probabilistic voltage stability assessment considering renewable sources with the help of the PV and QV curves. *IET Renew Power Gener.* Vol. 7. Issue 5. pp. 521-530. (2013). <https://doi.org/10.1049/iet-rpg.2012.0265>
- [23]. Zhou D.Q. *et al.* Online monitoring of voltage stability margin using an artificial neural network. *IEEE Transactions on Power Systems*. Volume: 25, Issue: 3, pp. 1566-1574. August 2010. [10.1109/TPWRS.2009.2038059](https://doi.org/10.1109/TPWRS.2009.2038059)
- [24]. R. Yan and T. K. Saha, "Investigation of voltage stability for residential customers due to high photovoltaic penetrations," *IEEE transactions on power systems*, vol. 27, no. 2, pp. 651-662, 2012.
- [25]. D. Q. Hung, N. Mithulananthan, and R. Bansal, "Integration of PV and BES units in commercial distribution systems considering energy loss and voltage stability," *Applied Energy*, vol. 113, pp. 1162-1170, 2014.
- [26]. H. Li, Y. Xu, S. Adhikari, D. T. Rizy, F. Li, and P. Irminger, "Real and reactive power control of a three-phase single-stage PV system and PV voltage stability," in Power and Energy Society General Meeting, 2012 IEEE, 2012, pp. 1-8: IEEE.
- [27]. E. Demirok, D. Sera, R. Teodorescu, P. Rodriguez, and U. Borup, "Clustered PV inverters in LV networks: An overview of impacts and comparison of voltage control strategies," in Electrical Power & Energy Conference (EPEC), 2009 IEEE, 2009, pp. 1-6: IEEE.
- [28]. J. Hernández, A. Medina, and F. Jurado, "Optimal allocation and sizing for profitability and voltage

- enhancement of PV systems on feeders," *Renewable Energy*, vol. 32, no. 10, pp. 1768-1789, 2007.
- [29].K. Le Dinh and Y. Hayashi, "Coordinated BESS control for improving voltage stability of a PV-supplied microgrid," in *Power Engineering Conference (UPEC), 2013 48th International Universities'*, 2013, pp. 1-6: IEEE.
- [30].K. Kawabe and K. Tanaka, "Impact of dynamic behavior of photovoltaic power generation systems on short-term voltage stability," *IEEE Transactions on Power Systems*, vol. 30, no. 6, pp. 3416-3424, 2015.
- [31].B. Tamimi, C. Cañizares, and K. Bhattacharya, "System stability impact of largescale and distributed solar photovoltaic generation: The case of Ontario, Canada," *IEEE transactions on sustainable energy*, vol. 4, no. 3, pp. 680-688, 2013.
- [32].R. Yan and T. K. Saha, "Investigation of voltage stability for residential customers due to high photovoltaic penetrations," *IEEE transactions on power systems*, vol. 27, no. 2, pp. 651-662, 2012.
- [33].R. Shah, N. Mithulananthan, R. Bansal, and V. Ramachandaramurthy, "A review of key power system stability challenges for large-scale PV integration," *Renewable and Sustainable Energy Reviews*, vol. 41, pp. 1423-1436, 2015.
- [34].Saidi, A.S.; Alsharari, F.; Ahmed, E.M.; Al-Gahtani, S.F.; Irshad, S.M.; Alalwani, S. Investigating the Impact of Grid-Tied Photovoltaic System in the Aljouf Region, Saudi Arabia, Using Dynamic Reactive Power Control. *Energies* 2023, 16, 2368. <https://doi.org/10.3390/en16052368>
- [35].Kundur P. *Power machine stability and manipulate*. McGraw- Hill Inc; 1994.
- [36].K. Turitsyn, P. Sulc, S. Backhaus, and M. Chertkov, "Options for control of reactive power by distributed photovoltaic generators," *Proceedings of the IEEE*, vol. 99, pp. 1063-1073, 2011.
- [37].R. Darbali Zamora , J. M. Arias Rosado, and Dr. A. J. Díaz Castillo, "Stability Analysis of Wind Energy Generation in the Electrical System of Puerto Rico", *International Conference on Renewable Energies and Power Quality (ICREPQ'14) Cordoba (Spain), 8th to 10th April, 2014 Renewable Energy and Power Quality Journal (RE&PQJ) ISSN 2172-038 X, No.12, April 2014.*
- [38].Mostafa H. Mostafa, Mostafa A. Elshahed and Magdy M. Elmarsfawy, "Power Flow Study and Voltage Stability Analysis for Radial System with Distributed Generation" *International Journal of Computer Applications (0975 – 8887) Volume 137 – No.9, March 2016.*
- [39].Taylor, C.W. *Power System Voltage Stability*; McGrawhil: New York, NY, USA, 1993.
- [40].Salma, A.; Eyad, F.; Ahmed, A.-S. Impact of Connecting Renewable Energy Plants on the Capacity and Voltage Stability of the National Grid of Jordan. In *Proceedings of the 8th International Renewable Energy Congress (IREC 2017), Amman, Jordan, 21–23 March 2017.*

Contribution of Individual Authors to the Creation of a Scientific Article (Ghostwriting Policy)

The authors equally contributed in the present research, at all stages from the formulation of the problem to the final findings and solution.

Sources of Funding for Research Presented in a Scientific Article or Scientific Article Itself

No funding was received for conducting this study.

Conflict of Interest

The authors have no conflicts of interest to declare that are relevant to the content of this article.

Creative Commons Attribution License 4.0 (Attribution 4.0 International, CC BY 4.0)

This article is published under the terms of the Creative Commons Attribution License 4.0

https://creativecommons.org/licenses/by/4.0/deed.en_US